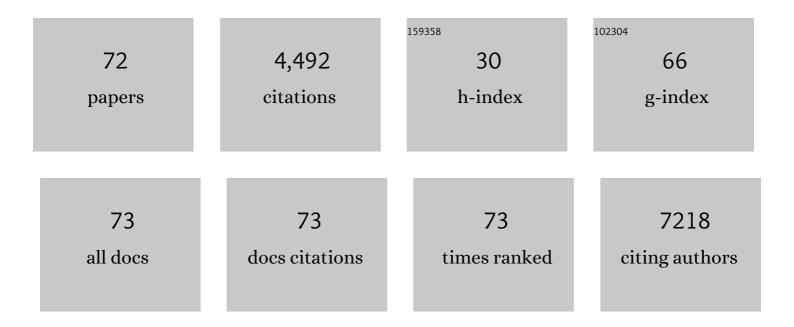
List of Publications by Year in descending order

Source: https://exaly.com/author-pdf/3558000/publications.pdf Version: 2024-02-01



Номения 7нон

#	Article	IF	CITATIONS
1	Nanoscale hydroxyapatite particles for bone tissue engineering. Acta Biomaterialia, 2011, 7, 2769-2781.	4.1	1,236
2	Various preparation methods of highly porous hydroxyapatite/polymer nanoscale biocomposites for bone regeneration. Acta Biomaterialia, 2011, 7, 3813-3828.	4.1	258
3	3D graphene/δ-MnO ₂ aerogels for highly efficient and reversible removal of heavy metal ions. Journal of Materials Chemistry A, 2016, 4, 1970-1979.	5.2	257
4	Bifunctional NH ₂ -MIL-88(Fe) metal–organic framework nanooctahedra for highly sensitive detection and efficient removal of arsenate in aqueous media. Journal of Materials Chemistry A, 2017, 5, 23794-23804.	5.2	230
5	The influence of biochar type on long-term stabilization for Cd and Cu in contaminated paddy soils. Journal of Hazardous Materials, 2016, 304, 40-48.	6.5	195
6	Efficient Synthesis of Furfuryl Alcohol from H ₂ -Hydrogenation/Transfer Hydrogenation of Furfural Using Sulfonate Group Modified Cu Catalyst. ACS Sustainable Chemistry and Engineering, 2017, 5, 2172-2180.	3.2	177
7	Wrinkled Surface-Mediated Antibacterial Activity of Graphene Oxide Nanosheets. ACS Applied Materials & Interfaces, 2017, 9, 1343-1351.	4.0	154
8	Pseudocapacitive deionization of uranium(VI) with WO3/C electrode. Chemical Engineering Journal, 2020, 398, 125460.	6.6	99
9	Dual-Mode SERS-Fluorescence Immunoassay Using Graphene Quantum Dot Labeling on One-Dimensional Aligned Magnetoplasmonic Nanoparticles. ACS Applied Materials & Interfaces, 2015, 7, 12168-12175.	4.0	95
10	Formation of BNC Coordination to Stabilize the Exposed Active Nitrogen Atoms in gâ€C ₃ N ₄ for Dramatically Enhanced Photocatalytic Ammonia Synthesis Performance. Small, 2020, 16, e1906880.	5.2	88
11	Green synthesis of phytochemical-stabilized Au nanoparticles under ambient conditions and their biocompatibility and antioxidative activity. Journal of Materials Chemistry, 2011, 21, 13316.	6.7	84
12	Ethanol introduced synthesis of ultrastable 1T-MoS2 for removal of Cr(VI). Journal of Hazardous Materials, 2020, 394, 122525.	6.5	79
13	Ultrasensitive DNA monitoring by Au–Fe3O4 nanocomplex. Sensors and Actuators B: Chemical, 2012, 163, 224-232.	4.0	76
14	Plasmon-tunable Au@Ag core-shell spiky nanoparticles for surface-enhanced Raman scattering. Nano Research, 2019, 12, 449-455.	5.8	72
15	Selfâ€Assembly Mechanism of Spiky Magnetoplasmonic Supraparticles. Advanced Functional Materials, 2014, 24, 1439-1448.	7.8	70
16	Fe3O4@Au nanoparticles as a means of signal enhancement in surface plasmon resonance spectroscopy for thrombin detection. Sensors and Actuators B: Chemical, 2015, 212, 505-511.	4.0	70
17	3D Fe ₃ O ₄ @Au@Ag nanoflowers assembled magnetoplasmonic chains for in situ SERS monitoring of plasmon-assisted catalytic reactions. Journal of Materials Chemistry A, 2016, 4, 8866-8874.	5.2	63
18	Europium-based infinite coordination polymer nanospheres as an effective fluorescence probe for phosphate sensing. RSC Advances, 2017, 7, 8661-8669.	1.7	62

#	Article	IF	CITATIONS
19	Fabrication of hierarchical iron-containing MnO ₂ hollow microspheres assembled by thickness-tunable nanosheets for efficient phosphate removal. Journal of Materials Chemistry A, 2016, 4, 14814-14826.	5.2	60
20	Selective Determination of Cr(VI) by Glutaraldehyde Cross-Linked Chitosan Polymer Fluorophores. ACS Sensors, 2018, 3, 792-798.	4.0	60
21	Three-dimensional honeycomb-like structured zero-valent iron/chitosan composite foams for effective removal of inorganic arsenic in water. Journal of Colloid and Interface Science, 2016, 478, 421-429.	5.0	55
22	Enhanced removal of trace Cr(VI) from neutral and alkaline aqueous solution by FeCo bimetallic nanoparticles. Journal of Colloid and Interface Science, 2016, 472, 8-15.	5.0	51
23	Ni/carbon aerogels derived from water induced self-assembly of Ni-MOF for adsorption and catalytic conversion of oily wastewater. Chemical Engineering Journal, 2020, 402, 126205.	6.6	51
24	Plasmon-Induced Photoluminescence Immunoassay for Tuberculosis Monitoring Using Gold-Nanoparticle-Decorated Graphene. ACS Applied Materials & Interfaces, 2014, 6, 21380-21388.	4.0	49
25	Magneto-plamonic nanoparticles enhanced surface plasmon resonance TB sensor based on recombinant gold binding antibody. Sensors and Actuators B: Chemical, 2017, 250, 356-363.	4.0	43
26	Selective Pseudocapacitive Deionization of Calcium Ions in Copper Hexacyanoferrate. ACS Applied Materials & Interfaces, 2020, 12, 41437-41445.	4.0	43
27	Multifunctional Magnetoplasmonic Nanomaterials and Their Biomedical Applications. Journal of Biomedical Nanotechnology, 2014, 10, 2921-2949.	0.5	38
28	Effective inspissation of uranium(VI) from radioactive wastewater using flow electrode capacitive deionization. Separation and Purification Technology, 2022, 283, 120172.	3.9	37
29	Microwave-assisted synthesis of magnetic Fe 3 O 4 -mesoporous magnesium silicate core-shell composites for the removal of heavy metal ions. Microporous and Mesoporous Materials, 2017, 242, 50-58.	2.2	35
30	Highly selective capacitive deionization of copper ions in FeS2@N, S co-doped carbon electrode from wastewater. Separation and Purification Technology, 2021, 262, 118336.	3.9	33
31	Small molecule induced self-assembly of Au nanoparticles. Journal of Materials Chemistry, 2011, 21, 16935.	6.7	29
32	Porous carbon nanosheets functionalized with Fe ₃ O ₄ nanoparticles for capacitive removal of heavy metal ions from water. Environmental Science: Water Research and Technology, 2020, 6, 331-340.	1.2	27
33	Flow-electrode capacitive deionization utilizing three-dimensional foam current collector for real seawater desalination. Water Research, 2022, 220, 118642.	5.3	27
34	Rapid detection of DNA by magnetophoretic assay. Sensors and Actuators B: Chemical, 2014, 198, 77-81.	4.0	26
35	Selective removal of Sr(II) from saliferous radioactive wastewater by capacitive deionization. Journal of Hazardous Materials, 2022, 431, 128591.	6.5	25
36	Self-assembled magnetoplasmonic nanochain for DNA sensing. Sensors and Actuators B: Chemical, 2014, 203, 817-823.	4.0	24

#	Article	IF	CITATIONS
37	Magnetic-Assembly Mechanism of Superparamagneto-Plasmonic Nanoparticles on a Charged Surface. ACS Applied Materials & Interfaces, 2015, 7, 8650-8658.	4.0	22
38	Synthesis of Gold Nanoparticles with Buffer-Dependent Variations of Size and Morphology in Biological Buffers. Nanoscale Research Letters, 2016, 11, 65.	3.1	22
39	Converting eggplant biomass into multifunctional porous carbon electrodes for self-powered capacitive deionization. Environmental Science: Water Research and Technology, 2019, 5, 1054-1063.	1.2	21
40	Enhancement of the visible-light photocatalytic activity of CeO ₂ by chemisorbed oxygen in the selective oxidation of benzyl alcohol. New Journal of Chemistry, 2019, 43, 7355-7362.	1.4	21
41	Pseudocapacitive desalination via valence engineering with spindle-like manganese oxide/carbon composites. Nano Research, 2021, 14, 4878-4884.	5.8	21
42	Intrinsic Pseudocapacitive Affinity in Manganese Spinel Ferrite Nanospheres for High-Performance Selective Capacitive Removal of Ca ²⁺ and Mg ²⁺ . ACS Applied Materials & Interfaces, 2021, 13, 38886-38896.	4.0	20
43	Highly sensitive detection of nitrite by using gold nanoparticle-decorated α-Fe ₂ O ₃ nanorod arrays as self-supporting photo-electrodes. Inorganic Chemistry Frontiers, 2019, 6, 1432-1441.	3.0	18
44	Cytotoxicity and Gene Expression in Sarcoma 180 Cells in Response to Spiky Magnetoplasmonic Supraparticles. ACS Applied Materials & Interfaces, 2014, 6, 19680-19689.	4.0	17
45	An adsorption–reduction synergistic effect of mesoporous Fe/SiO ₂ –NH ₂ hollow spheres for the removal of Cr(<scp>vi</scp>) ions. RSC Advances, 2016, 6, 27039-27046.	1.7	17
46	Synchronous removal of tetracycline and water hardness ions by capacitive deionization. Journal of Cleaner Production, 2021, 316, 128251.	4.6	17
47	Magnetically recyclable catalytic activity of spiky magneto-plasmonic nanoparticles. RSC Advances, 2015, 5, 56653-56657.	1.7	16
48	High-performance pseudocapacitive removal of cadmium via synergistic valence conversion in perovskite-type FeMnO3. Journal of Hazardous Materials, 2022, 439, 129575.	6.5	16
49	Metal (Co/Mo)–N bond anchor-doped N in porous carbon for electrochemical nitrogen reduction. Inorganic Chemistry Frontiers, 2021, 8, 1476-1481.	3.0	15
50	Enhanced Desalination Performance by a Novel Archimedes Spiral Flow Channel for Flow-Electrode Capacitive Deionization. ACS ES&T Engineering, 2022, 2, 1250-1259.	3.7	15
51	Synthesis of silver nanoparticles using analogous reducibility of phytochemicals. Current Applied Physics, 2016, 16, 738-747.	1.1	14
52	Improving the utilization rate of foliar nitrogen fertilizers by surface roughness engineering of silica spheres. Environmental Science: Nano, 2020, 7, 3526-3535.	2.2	14
53	Selective sodium(I) capture by olivine FePO4@C electrode in pseudocapacitive deionization: Mechanism and application. Desalination, 2022, 539, 115931.	4.0	14
54	Enhanced photocatalytic activity of a hollow TiO ₂ –Au–TiO ₂ sandwich structured nanocomposite. RSC Advances, 2016, 6, 18958-18964.	1.7	12

#	Article	IF	CITATIONS
55	Detection of anti-Neospora antibodies in bovine serum by using spiky Au–CdTe nanocomplexes. Sensors and Actuators B: Chemical, 2013, 178, 192-199.	4.0	11
56	Threeâ€Dimensional Nâ€doped Porous Carbon Derived from Monosodium Glutamate for Capacitive Deionization and the Oxygen Reduction Reaction. ChemElectroChem, 2018, 5, 3873-3880.	1.7	10
57	Oneâ€Step and Surfactantâ€Free Fabrication of Goldâ€Nanoparticleâ€Decorated Bismuth Oxychloride Nanosheets Based on Laser Ablation in Solution and Their Enhanced Visibleâ€Light Plasmonic Photocatalysis. ChemPhysChem, 2017, 18, 1146-1154.	1.0	9
58	In Vivo Study of Spiky Fe3O4@Au Nanoparticles with Different Branch Lengths: Biodistribution, Clearance, and Biocompatibility in Mice. ACS Applied Bio Materials, 2019, 2, 163-170.	2.3	9
59	Nitrogen-doped carbon nanotube encapsulated Fe ₇ S ₈ nanoparticles for the high-efficiency and selective removal of Pb ²⁺ by pseudocapacitive coupling. Environmental Science: Nano, 2022, 9, 2051-2060.	2.2	9
60	Simultaneous enhancement of Raman scattering and fluorescence emission on graphene quantum dot-spiky magnetoplasmonic supra-particle composite films. RSC Advances, 2015, 5, 81753-81758.	1.7	8
61	Novel Fe ₃ O ₄ nanoparticles-based DGT device for dissolved reactive phosphate measurement. New Journal of Chemistry, 2018, 42, 2874-2881.	1.4	8
62	Oxoacetohydrazideâ€functionalized cellulose with enhanced adsorption performance. Journal of Applied Polymer Science, 2016, 133, .	1.3	7
63	Removal of trace DNA toxic compounds using a Poly(deep eutectic solvent)@Biomass based on multi-physical interactions. Journal of Hazardous Materials, 2021, 418, 126369.	6.5	6
64	Copper nanocrystals anchored on an O-rich carbonized corn gel for nitrogen electroreduction to ammonia. Inorganic Chemistry Frontiers, 2020, 7, 3555-3560.	3.0	5
65	Antibacterial Activity of Graphene-Based Nanomaterials. Advances in Experimental Medicine and Biology, 2022, 1351, 233-250.	0.8	5
66	Silver-enhanced conductivity of magnetoplasmonic nanochains. Current Applied Physics, 2015, 15, 110-114.	1.1	4
67	Expandable photo-induced synthetic route to generate highly controlled noble metal nanoparticles. Current Applied Physics, 2015, 15, 1100-1105.	1.1	3
68	Evaluation of <i>β</i> -Amyloid Peptides Fibrillation Induced by Nanomaterials Based on Molecular Dynamics and Surface Plasmon Resonance. Journal of Nanoscience and Nanotechnology, 2015, 15, 1110-1116.	0.9	3
69	Calix[4]arene crown ether as an oriented linker for highly sensitive detection of zinc ions using a peptide probe. Analytical Methods, 2016, 8, 3959-3965.	1.3	2
70	A Novel Approach to Controlling CaCO ₃ Crystalline Assembly by Changing the Concentration of Poly(aspartic acid). Bulletin of the Korean Chemical Society, 2011, 32, 4027-4034.	1.0	2
71	Thermal behavior of surface plasmon resonance in dynamic suprastructure multilayer. Current Applied Physics, 2013, 13, 940-944.	1.1	1

Nanotechnology: A New Approach to Improve Orthopedic Implants. , 2012, , 401-443.

0